PHYSICAL REVIEW E **92**, 063008 (2015)

# Between giant oscillations and uniform distribution of droplets: The role of varying lumen of channels in microfluidic networks

Olgierd Cybulski,[1,*] Slawomir Jakiela,[1,2] and Piotr Garstecki[1,†]

[1]*Institute of Physical Chemistry, Polish Academy of Sciences, Kasprzaka 44/52, 01-224 Warsaw, Poland*

[2]*Department of Biophysics, Warsaw University of Life Sciences, Nowoursynowska 159, 02-776 Warsaw, Poland*

(Received 21 August 2015; published 8 December 2015)

The simplest microfluidic network (a loop) comprises two parallel channels with a common inlet and a common outlet. Recent studies that assumed a constant cross section of the channels along their length have shown that the sequence of droplets entering the left (L) or right (R) arm of the loop can present either a uniform distribution of choices (e.g., RLRLRL...) or long sequences of repeated choices (RRR...LLL), with all the intermediate permutations being dynamically equivalent and virtually equally probable to be observed. We use experiments and computer simulations to show that even small variation of the cross section along channels completely shifts the dynamics either into the strong preference for highly grouped patterns (RRR...LLL) that generate system-size oscillations in flow or just the opposite—to patterns that distribute the droplets homogeneously between the arms of the loop. We also show the importance of noise in the process of self-organization of the spatiotemporal patterns of droplets. Our results provide guidelines for rational design of systems that reproducibly produce either grouped or homogeneous sequences of droplets flowing in microfluidic networks.

DOI: 10.1103/PhysRevE.92.063008 PACS number(s): 47.55.D−, 47.60.Dx, 47.20.Ky, 47.54.−r

## I. INTRODUCTION

Here we demonstrate that *variation of the cross section of microchannels* along their length in microfluidic networks may determine the type of spatiotemporal patterns of droplets traveling through them. The simplest network is a microfluidic loop with two channels having a common inlet and a common outlet. We show that if these channels widen downstream, the droplets are distributed homogeneously over the loop. In contrast, narrowing of the lumen of the channels toward the exit of the loop produces long trains of drops flowing in alternation into each of the parallel ducts. This observation provides important insight into the simple one-dimensional models [1] that so far have been used to model the dynamics of flow of droplets in microfluidic networks. It may also be used to construct simple microfluidic systems that either "homogenize" or "chop" the sequences of drops. Finally, the observation may have biological connotations to the flow of blood in vascular networks.

Sequences of droplets flowing through—even simple—microfluidic networks often produce remarkably complex and beautiful patterns [2–5]. This complexity may be rooted in the interactions at many different length scales. Local interactions include collisions between neighboring droplets at the T junction [6–8] and capillary forces caused by a specific geometry of its walls [9]. However, the most important mechanism that gives rise to the complex dynamics is the long-range interaction associated with the changes in the pressure field that the droplets both introduce (by increasing the hydraulic resistance of the channel they occupy) and respond to (by choosing branches with higher inflow of the continuous liquid). The general dynamics of the flow of droplets can be analyzed with simple models of motion of point charges of resistance along the network of one-dimensional wires, as introduced by Schindler and Ajdari [1] and later used by multiple researchers in computer simulations [2–5,10–13] and analytical studies based both directly on the discrete model [3,10,14] and on its continuous generalizations [15,16].

Although simplified, the 1D model captures important aspects of collective interactions between the droplets, caused by the modification of the hydraulic resistance of the channels in which they flow. At diverging junctions droplets of size comparable or larger than the cross section of the channel can either split [17–20]—a scenario that we do not consider here—or enter the channel presenting momentarily the highest volumetric rate of inflow [6]. Since the rate of flow through a branch of a network is a function of resistance, the inflow of a droplet into a particular microchannel influences the trajectories of subsequent drops. The dynamics of flow of drops in networks has been studied in detail in a spectrum of microfluidic systems, ranging from the simplest, two-channel loops [2,3,10] to a long series of identical loops [5] to a successively bifurcating cascade of loops [15,21] to a large square grid of short channels [22]. Even the simplest nontrivial network, i.e., the simple loop exhibits highly complicated dynamics and complex dependencies on parameters [2–4,10–15,23] such as flow rates, intervals between droplets (or, equivalently, frequency of feeding droplets into the system), the additional hydraulic resistance incorporated by droplets, and length of arms of the loop. None of these papers has considered the effects of varying the cross section of the arms along their length on the dynamics of the system. This factor, however, is of practical relevance, both because of the finite precision of microfabrication that introduces undesired variation and of the simplicity of the deliberate introduction of such a variation in prototyping techniques. *As we show below, variation of the lumen along a fluidic branch in a network can have a critical influence on the global flow pattern.*

Any particular droplet entering the loop (see Fig. 1) may flow into either the left (L) channel or the right (R) channel. The sequence of these "choices" is a good descriptor of the dynamics of the system. This sequence can be conveniently

*olgierd.cybulski@gmail.com

†garst@ichf.edu.pl

 

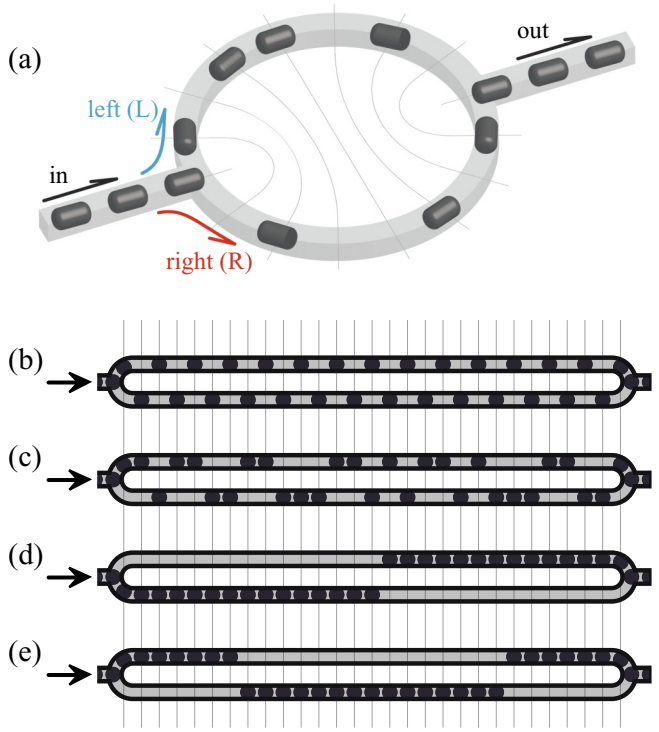


FIG. 1. (Color online) (a) A schematic rendering of a symmetric microfluidic loop. The thin gray lines mark the equidistant points in the parallel channels. [(b)–(e)] Exemplary momentary configurations of droplets in the loop for three different patterns: (b) perfectly homogeneous (chopped) sequence; (c) an intermediately chopped, random configuration; and [(d)–(e)] perfectly queued sequence at two instants.

encoded as a binary string, composed of these two (L and R) characters. Depending on the parameters, the additional hydraulic resistance carried by the droplets, the volumetric flow rate, and the frequency of dripping, this string can either be periodic or not. If it is periodic, then there are many possible patterns repeated infinitely [2]. Which of the many different stable states is selected, depends on the history of the system and on the initial conditions from which the flow started. If we define $N = N_L + N_R$ as the number of droplets in one period of the dynamics of the system, with $N_L$ and $N_R$ coding for the numbers of drops traveling through the left or right arm, then the number of distinct spatiotemporal patterns is given by

$$\Omega = \frac{(N_L + N_R - 1)!}{N_L!\, N_R!} \tag{1}$$

provided $N_L$ and $N_R$ are relatively prime numbers [2]. If they are not, then the simple combinatorial equation overestimates the number of patterns because it does not exclude redundant cyclic shifts. In that case the correct evaluation of $\Omega$ can be performed using Pólya enumeration, as it was shown by Glawdel *et al.* [3].

The theoretical model does not estimate the probability of falling into any single specific pattern when starting from random initial conditions. From computer simulations [2] we note that although some patterns are easier to obtain than other ones, the probabilities do not differ significantly. In different words, the basins of attraction of different patterns in the space of all possible initial conditions seem to be of comparable volume. The spectrum of all possible patterns includes interesting limiting cases, i.e., the ones that are maximally "homogenized" [Fig. 1(b)], and ones that are maximally "queued" [Figs. 1(d) and 1(e)]. Neither theory nor simulations suggest that these limiting patterns may be privileged over the vast majority of intermediate cases [as in Fig. 1(c)]. The probability of any of the limiting sequences to occur in a randomly started experiment should be of the order of $1/\Omega$—a very small number for large $N$ (for example, for $N = 30$, $1/\Omega < 10^{-6}$).

Thus, on the basis of the existing theory, one would not expect any of the patterns (including the chopped or queued pattern) to prevail in the experiments. The goal of this article is to explain why this is not necessarily true in a real experiment and how a small modification of the system may enforce or suppress the tendency to either homogenize or queue the distribution of droplets in networks.

## II. EXPERIMENTAL MOTIVATION

Several experimental reports confirm the predictions of the simplest model [1] in systems with relatively short parallel channels [2,3,10,14,15,23]. The existence (i.e., the appearance and stability) of all predicted patterns for $N_L = N_R = 4$ ($\Omega = 10$) and for smaller $N_L$, $N_R$ was demonstrated in Ref. [2]. Adjacent bands of regular (periodic) and irregular dynamics as well as stepwise dependence of the period on the frequency of dripping were reported in Refs. [2,3,10,14,23]. All these results agreed with simulations and analysis based on Schindler's model [1]. In all the experiments it was observed that after some number of repetitions the pattern may spontaneously switch into a different one; such a behavior was attributed to fluctuations of experimental conditions, i.e., to the experimental noise.

The fundamental assumptions of the ideal model [1] should be even better fulfilled in systems comprising long channels—i.e., channels that can accommodate hundreds of droplets—because such systems are closer to the approximation of single lane ducts. Also the role of noise, which should be proportional to the effects associated with the flow of a single droplet, should decrease in relation to the overall dissipation in a large system. From this, and from the fact that the number $\Omega$ of possible trajectories explodes in a factorial fashion with $N$, one can expect that in a large system the chance of observing any particular pattern, as well as the chance of coming back to a pattern once abandoned (due to noises or disturbances) should be vanishingly small.

In order to verify these predictions, we performed an experiment using the same technology as in the recent experiment that confirmed the ideal model [2]; the only difference was that the two channels forming the loop were much longer (about 180 mm, more than 400 times longer than they were wide). These channels could comprise hundreds of droplets at a time. Quite surprisingly, our predictions proved completely wrong: Instead of observing an erratic creeping of the system over the whole space of allowed configurations, the system always settled into the "maximally queued" pattern, as in Figs. 1(d) and 1(e). This behavior was neither dependent on the frequency of feeding the droplets into the loop nor on the

droplet size: As long as droplets were able to pass the junction without breaking up, the long queues always appeared. We also observed that this behavior did not depend on the method of generation of droplets: We reproduced the same results with (i) a well-tuned droplet on demand (DOD) system [24] that produced a sequence of equally spaced monodisperse droplets, (ii) with an improperly vented DOD valves producing droplets with a considerable variation in their size, and even (iii) without an active control of the generation of drops, when both their volume and spacing between the drops changed in response to the changing load of the system. Although initially (if starting from the empty channels) the droplets tended to form patterns similar to these from Fig. 1(b) and Fig. 1(c) (i.e., "chopped"), the long trains of drops always appeared within minutes and persisted, no matter how long the experiment ran.

Puzzled by this result we considered the following questions: (i) Can the observed dynamics be explained within the ideal model? If not, (ii) then what kind of nonlinearities or other corrections should be taken into account to find the possible reason in a minimalistic yet plausible way? If yes, (iii) then why there was not a single report of this problem in the literature related to a wide range of simulated microfluidic networks?

The last question proved most helpful in searching the literature for aspects that have not been considered. Most reports on modeling flow of drops in microfluidic networks focus on systems with channels of varied lengths yet always of constant cross section. This seems a natural choice, first, for the clarity of analysis and, second, because it is typical and experimentally easiest to prepare chips with (nominally) constant height and width of the channels. If the cross section of the channels were truly constant, then it would be necessary to look for the reason of queuing in subtle and little known effects, such as, e.g., distance-dependent hydrodynamic interactions between droplets [25]. From auxiliary measurements we found that this effect was negligible under the conditions of the experiment described here. Moreover, we observed the queuing dynamics regardless of interdroplet separation even though the cooperative effects, if any, should be negligible for large intervals between droplets. We thus focused further analysis on the effects of a variable cross section on the dynamics of flow of drops through networks. An extra reason to follow this path was the fact that both the process of milling long channels and bonding chips in a hot press are prone to systematic deviations of the depth of channels—due to thermal expansion of spindle in milling and due to nonuniform temperature and pressure field in a press.

## III. THEORY AND SIMULATIONS

In the case of flow of simple, Newtonian fluid, the variation of cross section of the channel along its length cannot produce any variation in time. Even though the local pressure gradient depends on the local geometry, any given spot along the channel is always filled with the same liquid. Yet, when the fluid is complex and nonhomogeneous, such as e.g., a suspension of droplets, the local pressure gradients will depend on the content of the channel at any given point. In consequence also the total hydrodynamic resistance of the channel may depend on the position of droplets along its length and change in time. Even for a simple liquid the hydrodynamic resistance ($R$) is very sensitive to changes in the transverse dimensions (say, $d$) of the channel. According to the Hagen-Poiseuille law, reduction of the diameter of the duct from $d$ to $\gamma d$ ($\gamma < 1$) changes the resistance by a factor $\gamma^{-4}$. In the case of an immiscible droplet, this scaling is much more complicated: Not only does the droplets' cross-sectional area decrease by a factor $\gamma^2$, but also its length increases by a factor $\gamma^{-2}$. Further, its linear speed of flow must—by conservation of mass—increase approximately $\gamma^{-2}$ times. In a very rough approximation, the elongated droplet of high viscosity may be described as a slug of Hagen-Poiseuille flow of the length $\Delta l$, with effective viscosity $\eta_{\text{eff}}$ being the difference between the viscosity of the discrete and the continuous liquids, $\eta_{\text{eff}} = \eta_d - \eta_c$. Within this crude approximation, the resistance introduced into the channel by a droplet is proportional to $\Delta l/d^4$, and the change associated with reduction of the diameter of the pipe scales as $\gamma^{-6}$. For example, a mere 10% decrease of the diameter of the pipe results in a 23% increase in the length of the drop and in almost doubling of the resistance the droplet adds to the resistance of the channel. The above estimation is rough: The only important insights that we draw from it are that (i) the total resistance to flow in a microfluidic channel increases when droplets move into a narrower segment and that (ii) this effect may be significant. Instead of dealing with unknown dependence of these additional resistances on a cross section of channels, flow rates, and sizes of droplets, we simply assume that the resistance of a droplet is given by $r_{\text{up}}$ in the upstream segments and $r_{\text{down}}$ in the downstream segment (see Fig. 2). As the resistances of individual droplets may differ (due to emulated noise in simulations or polydispersity of droplets in experiments), we will instead use the ratio of

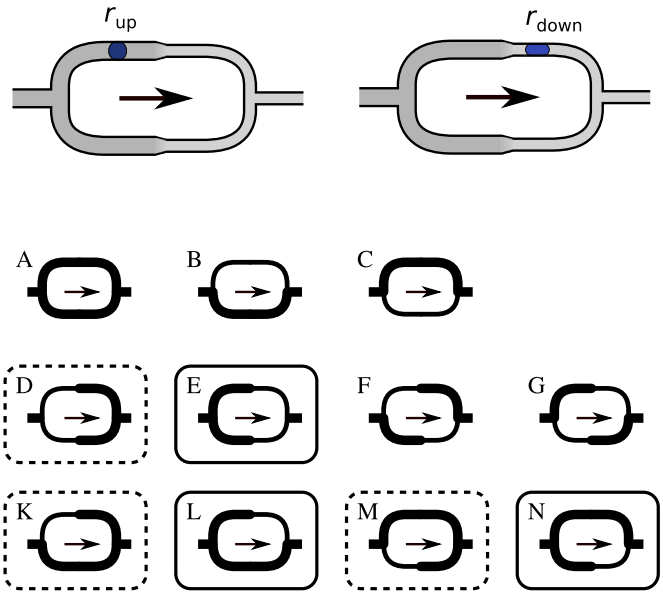


FIG. 2. (Color online) Upper panel: Change of the shape and additional resistance of a droplet due to the varying cross section of channels. Lower panel: Modifications of the asymmetric loop to be tested with respect to queuing. Thin lines correspond to the segments of modified cross section—narrower than the other channels. Configurations indicated by solid frames induced queuing, dashed frames—chopping (suppression of queues).

these resistances:

$$\alpha = \frac{r_{\text{down}}}{r_{\text{up}}}, \tag{2}$$

having in mind that $\alpha$ may be equal to $r_{\text{narrow}}/r_{\text{wide}} > 1$ in loops narrowing downstream or $r_{\text{wide}}/r_{\text{narrow}} < 1$ in the opposite case.

Networks comprising segments of slightly different cross sections may be simulated without adding new features to the Schindler's model; it is enough to divide channels into subsections, each having its own geometry and its own resistance multiplier for droplets, and simulate the divided channels as being connected in series. The notion of slightly different cross sections requires clarification: We use this term to emphasize the fact (or assumption) that the dynamics of the system is dominated by collective effects of additional resistance carried by droplets and not by local effects of passing through the junctions between channels of different cross section. The presence (and motion) of droplets in such a section involves additional pressure drop due to capillary effects [26]. This transient pressure drop could be taken into account for reliable analysis and simulation, but for simplicity—since we only want to demonstrate that the queuing phenomenon may be related to a nonconstant cross section of channels—we will neglect it.

Therefore, using the simple model and neglecting capillary effects on channel contractions, we tested several simple modifications of a classic asymmetric loop. We introduced narrowed sections of channels equal to either half or the whole length of the single parallel section and we varied their location. The bottom panel of Fig. 2 shows the configurations that we tested. The segments marked with the thin line are narrower than those drawn with the wide solid line.

We observed that these systems varied strongly in their tendency to form long queues: Some of the geometries exhibited queuing (. . . LLLLRRRR . . . ), some seemed to suppress queues (i.e., to prefer frequent switching between L and R), and the behavior of others depended strongly on the initial conditions. Specifically, geometries B and C were neutral in the sense, in that they exhibited the full range of combinatorial patterns, as in the unmodified case A. Geometries D, K, and M tended to suppress queuing—even if the simulation had been started from a "perfect queue." The cases F and G were difficult to classify; for some specific sets of starting configurations the preferred patterns were "queuelike" yet the length of queues were far from maximum. Finally, L, N, and, most of all, E formed queues of the maximum possible length (i.e. longer than half of the length of the channels).

### A. The onset of oscillations

In the following analysis we focus on systems with narrowed sections positioned at the downstream half of the parallel channels (as in Fig. 2, case E). For simplicity, we consider a symmetric loop with both parallel sections of equal length and having identical segments of reduced lumen. Examples of the process described here are shown in Fig. 3—the three snapshots of experiment (details of the experiment are provided in Sec. IV) and corresponding computer simulation illustrate the evolution of patterns at the beginning (just after first droplets reach the end of the loop that was initially filled solely by the continuous liquid), in an intermediate state (as the queues start grow), and with fully developed queues.

When the first droplet enters the (initially empty) loop, it may flow into any of the arms. In real systems the choice is predetermined by inevitable deviations from the perfect symmetry of channels and T junctions, and in simulations the decision must result from the details of algorithm and from the finite precision arithmetics. This droplet increases the hydraulic resistance of the chosen channel by $r_{\text{wide}}$. The subsequent droplet will then choose the opposite branch, and, once it flows in, it increases the resistance of the second channel by the same amount, balancing the rates of flow through each of the arms. If the symmetric loop did not comprise the narrowed sections, this simple mechanism would lead to a "chopped" state with alternating L/R trajectories of the droplets. This uniform configuration of droplets can be sustained *ad infinitum*: As a drop leaves a branch and decreases its resistance, the next droplet will flow to the same arm of the loop. Interestingly, the introduction of a narrowing at the downstream termini of the arms destroys the stability of the "chopped" state. When a droplet passes into the narrowed section, the drops' contribution to the resistance of the channel increases from $r_{\text{wide}}$ to $r_{\text{narrow}}$, so the excess of flowing resistance in this branch is amplified by a factor $\alpha = r_{\text{narrow}}/r_{\text{wide}}$ [see Eq. (2)]. This increase must be compensated by new droplets entering the opposite branch and since they introduce smaller resistive contributions, one droplet does not balance the inequality of resistances of the two branches. The combination of the change in the resistive charge of the droplets and the delay between a decision taken at the inlet and its amplification at the narrowing, provides for the instability of the chopped states: The perturbation will be larger and larger with each cycle, finally leading to the oscillation of the maximum possible amplitude.

Figure 4(a) shows an example of development of queues in a simulation with $\alpha = 2.44$. In Fig. 4(b) we graphed a zoom on the dynamics of the system in the fully developed queued state. The top panels of these plots show a discrete function taking on two distinct values: $+1$ if a droplet flows to the right arm (R) and $-1$ if to the left (L).

Integrating this signal over time leads to the function $C(t)$ plotted in the second panel of Fig. 4(a). This function may be interpreted as the difference between the numbers $C_R(t)$ and $C_L(t)$ of droplets that flew to the right and left channels, respectively (from the beginning of the simulation). Due to the symmetry of the loop, both $C_L(t)$ and $C_R(t)$ increase with the same average speed and $C(t) = C_R(t) - C_L(t)$ oscillates around zero. However, the amplitude of changes of $C(t)$ provides a measure of queuing. In a perfectly chopped state $C(t) \in (-1,1)$ because droplets enter the channels in alternation. In a queued state $C(t)$ departs far from zero because long trains of droplets follow the same trajectory. We normalized the rates of flow through each of the branches by the total volumetric flow rate—hence the rates of flow through each of the two branches oscillate around the value of 0.5 [third panel of Fig. 4(a) and second panel of Fig. 4(b)]. At bottom panels we also plot the numbers of droplets residing in the right or left arm of the loop at any given instant of time,

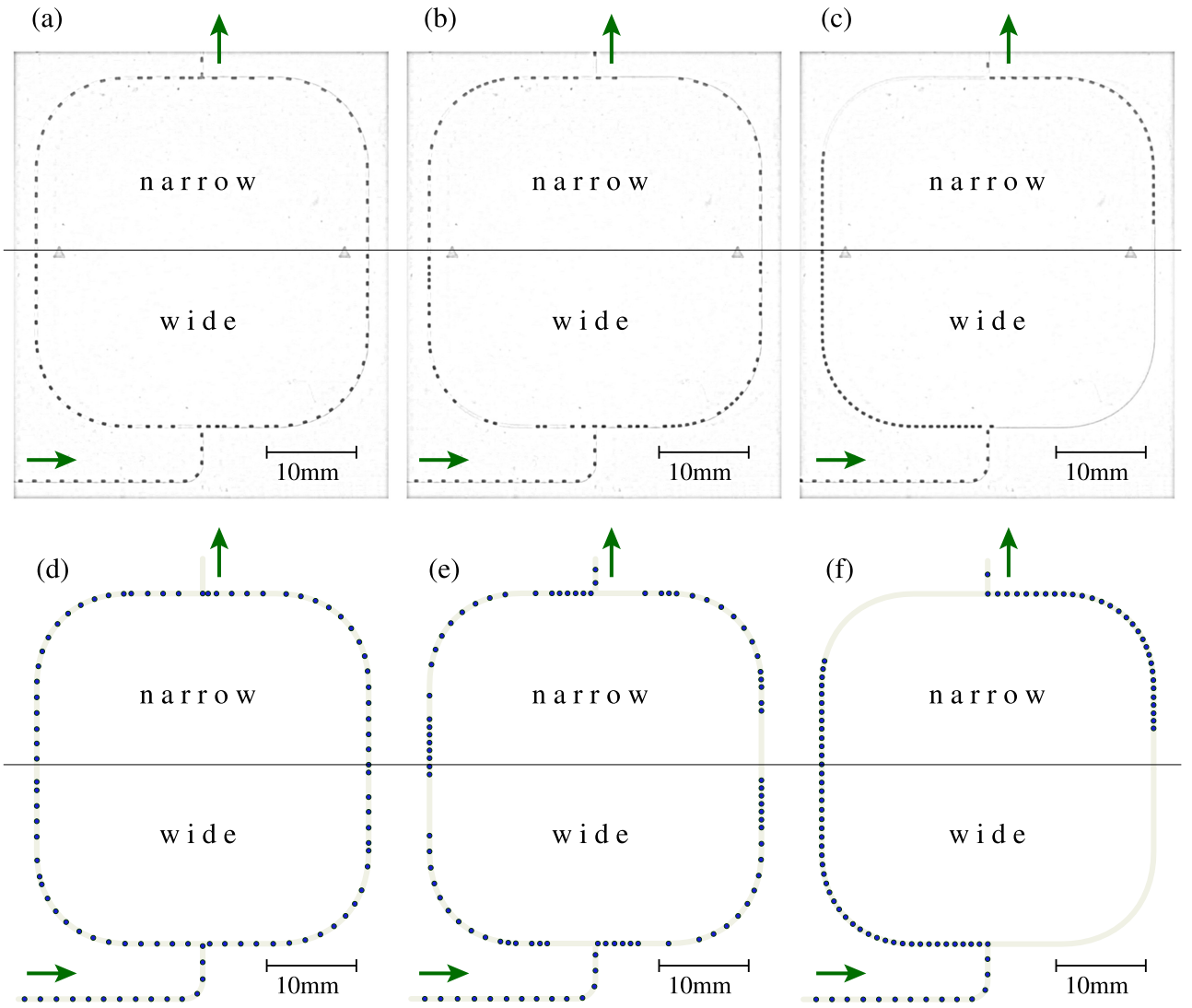


FIG. 3. (Color online) Top panel [(a)–(c)]: Photographs of the experiment with evolving pattern of droplets in the loop with narrowing channels: (a) at the beginning, (b) intermediate, and (c) stationary states. Bottom panel [(d)–(f)]: Snapshots of corresponding simulations.

and the corresponding numbers of droplets in the initial (not narrowed) sections.

Since the simulation starts with empty channels, at the beginning droplets enter both channels in an alternating manner; both trains of droplets move downstream their arms at almost the same speed and reach the narrow segments almost in the same time and then, similarly, they reach the end of the loop. In the absence of any noise, this behavior could continue infinitely; locking the system in this metastable state is possible because the loop is symmetric. The onset of queuing requires a small perturbation or a finite level of noise. We will discuss the role of noise in detail in the next section. Interestingly, the growth of queues is not monotonic. Usually two or more shorter chains grow independently to finally combine into the queue of the terminal (maximum) length.

At first sight the fully established queued state in the system comprising the narrowed sections [Fig. 3(c), Fig. 3(f), Fig. 4(b), and Fig. 4(c)] resembles the queued pattern from Figs. 1(d) and 1(e) in a symmetric loop without any constrictions. There are, however, important differences. First, in the system without constrictions, the queued pattern is solely *one of multiple* degenerated stationary states and it thus can be easily destroyed by a random perturbation. In the system with the narrowed sections the queued state is the *only* stable stationary state and is robust against noise. Second, in the constant cross-section system both the number of droplets and the rates of flow are—to within a single droplet and its effect of the flow rate—constant in each branch. In the narrowing loop both of these quantities change significantly within each cycle. The magnitude of these changes increases with the degree of modification: The narrower the cross section of the modified segments, the larger these deviations. Moreover, exactly these cyclic variations contribute to the stability of the queued state: The large momentary differences of the flow rates determine the trajectories of drops entering the loop. Random perturbations may change the trajectories of the droplets only at the ends of the queues—as only at the moment of switching the flow rates in both arms are of similar value. Third, in the unmodified system, the droplets formed mutually complementary patterns in the two arms:

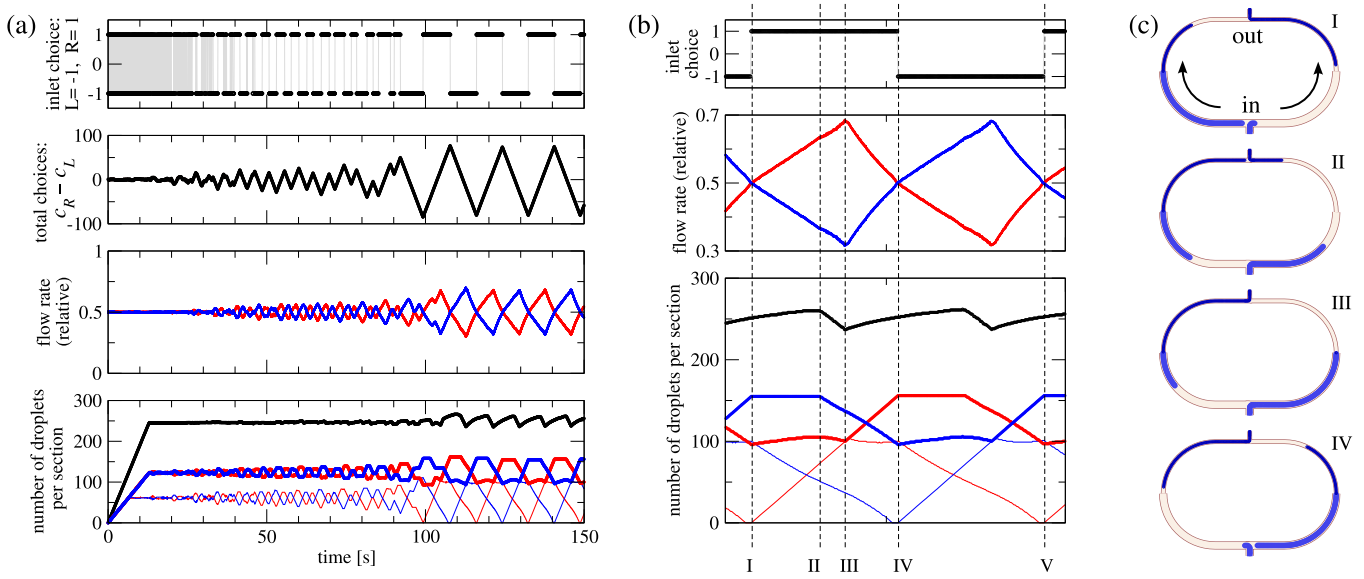


FIG. 4. (Color online) Onset of oscillations in the symmetric loop comprising sections of narrowed channels from a computer simulation. (a) Time dependence of key variables in the simulation started from an empty system. The "inlet choice" signal (top panel) is assigned the value $+1$ if a droplet flows to the right channel and $-1$ if to the left. The second panel plots the difference $C(t) = C_R(t) - C_L(t)$ between the number $C_R(t)$ of droplets that had chosen the right channel and $C_L(t)$ for the left one. The third inset shows the flow rates through the arms (solid blue for the left channel and dashed red for the right one) normalized by the total volumetric flow through the loop. The fourth chart plots the momentary numbers of droplets in the whole loop (thick black solid line), in the right arm (thick solid red line), and in the left arm (thick dashed blue line). The thin lines show the number of drops in the initial (not narrowed) sections of these channels. (b) Magnified part of the same plots, comprising single, fully established cycle of oscillation, with characteristic instants of time marked by roman numerals. (c) Positions of droplet queues at these instants: (I) Due to a long series of droplets previously loaded into the left channel, its resistance becomes higher than of the right channel; new droplets start to enter the right channel; (II) the front of the queue in the left channel reaches the end of the loop; (III) the front of the queue in the right channel approaches the narrowed (and momentarily empty) section; the flow rate in the right channel achieves maximum value, while rate of flow in the left channel is minimum; (IV) symmetric to (I); (V) completion of the cycle—the system comes back to the configuration (I).

The positions of droplets in one channel matched positions of the gaps in the second (see the thin lines in Fig. 1). In the modified system this rule no longer holds—the lengths of the queues are substantially longer than half the length of each channel [see Fig. 3(c), Fig. 3(f), and Fig. 4(c)] and are not complementary. For example, in configuration II in Fig. 4(c) the queues from the two arms flow into the outlet at the same time, possibly leading to mutual collisions of droplets leaving each of the arms. This lack of complementarity causes both the total number of droplets in the loop and the pressure drop at constant flow rate conditions (or the flow rate in constant pressure) to vary within each cycle.

### B. Suppressing oscillations

If, on the other hand, narrowed sections are positioned at the upstream half of the parallel channels (as in Fig. 2, cases D, K, and M), the oscillations not only do not occur but also will be suppressed (if the queued state is artificially created by the initial configuration). It means that the same loop, traveled by the same sequence of droplets (i.e., with the same flow rate, volumes, and separation between droplets) will behave completely differently after switching the direction of flow. In particular, reversing the direction of flow in the system shown in Fig. 3 will lead to patterns with a low number of the same choices (i.e., LL or RR) in order. Mathematically, the reversal of the direction of flow means changing $\alpha$ [see Eq. (2)] from $r_{\text{narrow}}/r_{\text{wide}}$ to $r_{\text{wide}}/r_{\text{narrow}}$. If $\alpha > 1$ corresponds to amplifying fluctuations of "flowing resistance" and growing oscillations to highest available amplitude, then reversal of the flow means that the oscillations become damped. Nevertheless, it does not simply mean the reversal of the direction of evolution nor the substitution of the target of the evolution from perfect queuing (...LLLLRRRR...) to perfect chopping (...LRLRLRLR...). For $\alpha > 1$ the evolution leads to uniquely defined state of the perfect queues (perhaps with some minor deviations only at the very ends of the queues, caused by high levels of noise). In contrast, reversing the flow ($\alpha < 1$) does not lead to a single, unique state but to a family of microstates that distribute droplets between two arms more or less homogeneously. These microstates can easily mutate into each other because (in contrary to the queues for $\alpha > 1$) the system is always almost balanced—the difference of flow rates between arms is as small as the effect of single droplets, so a random permutation may be located in any spot along the sequence. Thus in the case of $\alpha < 1$ the evolution seems to escape from queue rather than run towards any particular, highly chopped pattern.

Although the confirmation of this finding in computer simulation is straightforward, as the simulation may be started from any initial configuration of droplets, experimental tests require more caution. Typical experiment starts from empty

loop and then continue to more or less uniform distribution of droplets. Therefore, in order to prove that queuing is suppressed, the queue must be created artificially. We did it by freezing the flow in one of the arms (by placing a piece of dry ice above the chip), so droplets could not enter the blocked channel. After removing the ice and melting the frozen oil, the channel was again open for flow, but the artificially created queue was not stable and evolved to a chopped state after several cycles [see the details in Sec. IV and in particular those in Fig. 7(b)].

### C. Effects of noise and of geometry on formation of queues

As discussed above, the onset of queuing usually requires a random perturbation that may change the "ideal" pattern of L and R choices. In a small experimental systems it is likely that the experimental noise is too small to induce a change of the stationary pattern of trajectories. In a large system, with a large number of droplets, their time of residence in the parallel arms is long enough for small perturbations to accumulate. In simulations, we added artificial noise by randomizing the intervals between subsequent droplets entering the loop and by randomizing the volume and charge of resistance of the droplets. Intervals between the droplets and their resistances were drawn from a symmetric triangular distribution centered at the required mean value with ranges given as a specified percentage of the mean. For example, in the simulations plotted in Fig. 3(d)–Fig. 3(f) and Fig. 4, the emulated noise was $\pm 10\%$ of droplet resistance and $\pm 10\%$ of the interdroplet interval. The standard deviations of the corresponding distributions were $\sqrt{6}$ times smaller, i.e., 4.1% of a mean value.

We used simulations to test the minimum amplitude of noise needed for initiating the process of queuing. In order to quantify how quickly the queues grow, we constructed a quantity reflecting the extent to which the state of the system resembled a "perfect queue" comprising a maximum number of droplets in a row. An exact estimation of this maximum length is not straightforward, but it is of the order of the maximum number of droplets in the whole loop. This number is also difficult to calculate exactly yet, using the "mean-field approximation" for an unmodified loop, we obtain the following estimation:

$$\bar{N}_L = \frac{L_L \bar{f}_L}{\bar{v}_L}, \quad \bar{N}_R = \frac{L_R \bar{f}_R}{\bar{v}_R}, \tag{3}$$

where $\bar{N}_i$ is the average number of droplets, $L_i$ is the length, $\bar{f}_i$ is the average frequency of entering droplets, and $\bar{v}_i$ is the average velocity in the $i$-th channel ($i = L$ or $R$). For a symmetric, unmodified loop ($L_L = L_R = L$) the corresponding values are equal:

$$\bar{v}_L = \bar{v}_R = \frac{Q}{2A}, \quad \bar{f}_L = \bar{f}_R = \frac{f}{2}, \tag{4}$$

$$\bar{N}_{\text{tot}} = \bar{N}_L + \bar{N}_R = \frac{2ALf}{Q}, \tag{5}$$

where $Q$ is the total volumetric flow rate, $f$ is the frequency of feeding droplets into the loop, and $A$ is the cross-sectional area of the channels. Here we assume that $A = wh$ is constant along channels while the increase of the hydraulic resistance introduced by the droplets results from modification of the aspect ratio $w/h$ of the width ($w$) and height ($h$) of the channel. This way the resistance of droplets is changed, but their length, separation and velocity are not.

The "perfect queue" should contain at least $\bar{N}_{\text{tot}}/2$ droplets flowing one after another into the right channel and the same number of drops then flowing into the left arm. We monitor the interval required for the onset of the oscillations as the interval from the start of simulation until the first occurrence of $\bar{N}_{\text{tot}}/2$ subsequent droplets following through the same channel.

Figure 5 shows the time required for the onset of oscillations as the function of $\alpha$ [defined in Eq. (2)]. We run the simulations keeping constant flow rate and varying the frequency of feeding droplets into the loop, the volume of the droplets, and the amplitude of noise (same for the intervals between the drops and the resistance they carried). We note that the time

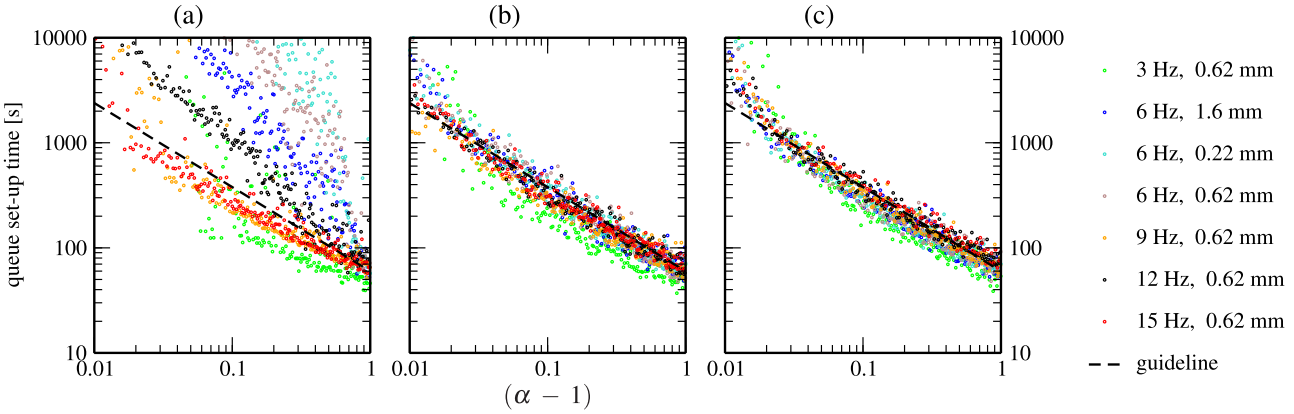


FIG. 5. (Color online) Time of approach to a fully developed oscillation, as a function of the factor of increase of the hydrodynamic resistance of droplets entering the narrowed section of the channel. The three graphs differ in the noise level: (a) 3%, (b) 10%, and (c) 30% of the mean interval between drops and of the mean resistance of the drops. Simulations were performed for varied frequency (Hz) of feeding droplets into the loop and for varied resistance equivalent length (mm) of the droplets (see the legend). The dashed line is a power function proportional to $(\alpha - 1)^{\beta}$, with $\beta = 0.8$. All simulations were performed for a symmetric loop with arms of length 20 mm, divided into two equal segments of different cross section. The linear velocity of feeding droplets (in the common inlet channel) was set to 3.1 mm/s. The resistance equivalent lengths are given with respect to the initial (wide) segments of the loop.

required for the onset of oscillations depends very weakly on the resistance of droplets and on the frequency of drops entering the loop. It is possible that this dependence, visible especially at the low noise level on the left graph in Fig. 5, results mainly from the hidden influence of these quantities on the overall fluctuations in the flux of hydrodynamic resistance through the system. This is because we define the amplitude of the noise in relation to the resistance of droplets or frequency of feeding the droplets; increasing these parameters increases also the amplitude of fluctuations. These effects play a crucial role when the level of noise is small and $\alpha$ is too small to induce permutation of a pattern without a random perturbation.

### D. Effects of noise and of geometry on the quality of queues

Apart from the onset of oscillations, the "quality" of queues is also of interest. In order to test the stability of the queued states we monitored to what extent the state of the system resembled the perfect queue. We note that the sole number of identical subsequent decisions overlooks states that differ only very slightly from a "perfect queue." For example, for $\bar{N}_{\mathrm{tot}}/2 = 12$ the string LLLLLLLRLLLLLLL will be rejected despite more than 12 L choices almost in a row. In order to take into account these imperfections we introduced the following criteria:

(i) The amplitude of oscillation, defined as the difference between maximum and minimum of value of $C(t)$ within a cycle. To avoid ambiguities in identification of the cycle and calculating its length, we use its rough estimate $\bar{N}_{\mathrm{tot}}$.

(ii) The number of changes from L to R or vice versa during the cycle. Perfect queuing should yield 1 or 2 changes depending on whether the actual length of the cycle is longer or shorter than the estimate $\bar{N}_{\mathrm{tot}}$. In contrast, perfectly chopped state (in a symmetric loop) produces maximum possible value, which is equal to the length of the cycle.

Figure 6 shows how these two measures of queuing depend on the factor $\alpha$, defined in Eq. (2). Each point in these graphs represents a data point from a simulation, started from random initial conditions and recorded after a long time (10 000 droplets). In these simulations $\bar{N}_{\mathrm{tot}} = 116$. We varied the level of noise (0, 10, or 90%) and $\alpha$, with all the other parameters held constant. $\alpha < 1$ corresponds to loops comprising downstream halves of the two parallel channels wider (less resistant) than the upper ones, and $\alpha > 1$ codes for systems with narrowed sections. At moderate level of noise (10% or 4.1% in terms of the standard deviation) both criteria indicate perfect queuing already for values of $\alpha$ as close to 1 as just $\alpha > 1.02$. The slight increase of the amplitude of oscillations is due to the hidden dependence of both $N_{\mathrm{tot}}$ and the actual length of the queues on the cross-sectional area of modified sections (changing together with $\alpha$). For the large level of noise (90%) and $\alpha > 1$, there are visible imperfections in the queues, increasing for $\alpha \approx 1$. In stark contrast, when the downstream sections provide for a lesser resistance introduced by the droplets than the upstream sections of the channels (i.e., for $\alpha < 1$), queuing is suppressed, regardless of the level of noise. Interestingly, at a high level of noise the number of changes per cycle is close to half its length, just as if the sequence of L/R choices was random. On the other hand, the amplitude of oscillation measured for real random binary

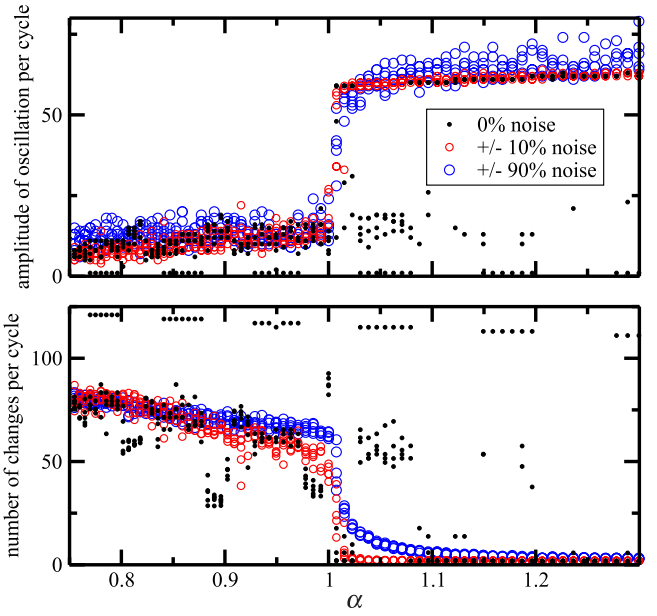


FIG. 6. (Color online) The amplitude of oscillations and the number of changes of the trajectories of droplets within one cycle as a function of $\alpha$. Data shown for long, randomly initialized simulations of the symmetric loop containing about 120 droplets. The amplitude of oscillations assumes high values in states with long queues, while the number of changes of the trajectories assumes small values in the queued state. From the graphs it is clear that when the downstream halves of the channels induce higher hydrodynamic resistance of droplets ($\alpha > 1$) queues form, while the reduction of the resistance of introduced by the droplets in the downstream sections ($\alpha < 1$) suppress queues. This behavior is stabilized by a moderate level of noise.

strings (resulting from the Bernoulli process, as repeated coin flipping), is higher than that recorded in the simulation. We attribute this fact to the mechanism of suppression of long queues (see Sec. III B).

It is also very interesting to note that in the absence of noise (0%) all the above regularities become less evident. For example, for $\alpha > 1$ queuing may be overcome by regular memorized patterns [2] (notice the characteristic structure of bands in the dependence on $\alpha$). Locking the system in a "perfectly chopped" state is still possible, although it requires very special initial conditions, as starting from the empty loop. Interestingly, suppression of long queues in widening channels ($\alpha < 1$) is still efficient in the absence of noise: Even if simulation starts from perfect queues, they disappear. This is because the imbalance needed for changing a pattern comes collectively from all droplets if starting from a queue and from one droplet only (plus fluctuations or noise) if starting from the chopped pattern (as well as from the empty loop).

## IV. EXPERIMENTAL RESULTS

Our predictions have been fully confirmed in experiments. We manufactured four different microfluidic chips, each comprising two kinds of channels: "narrow" and "wide." Despite these names, used for consistency, the channels, milled in a slab of extruded polycarbonate (Makrolon) and sealed

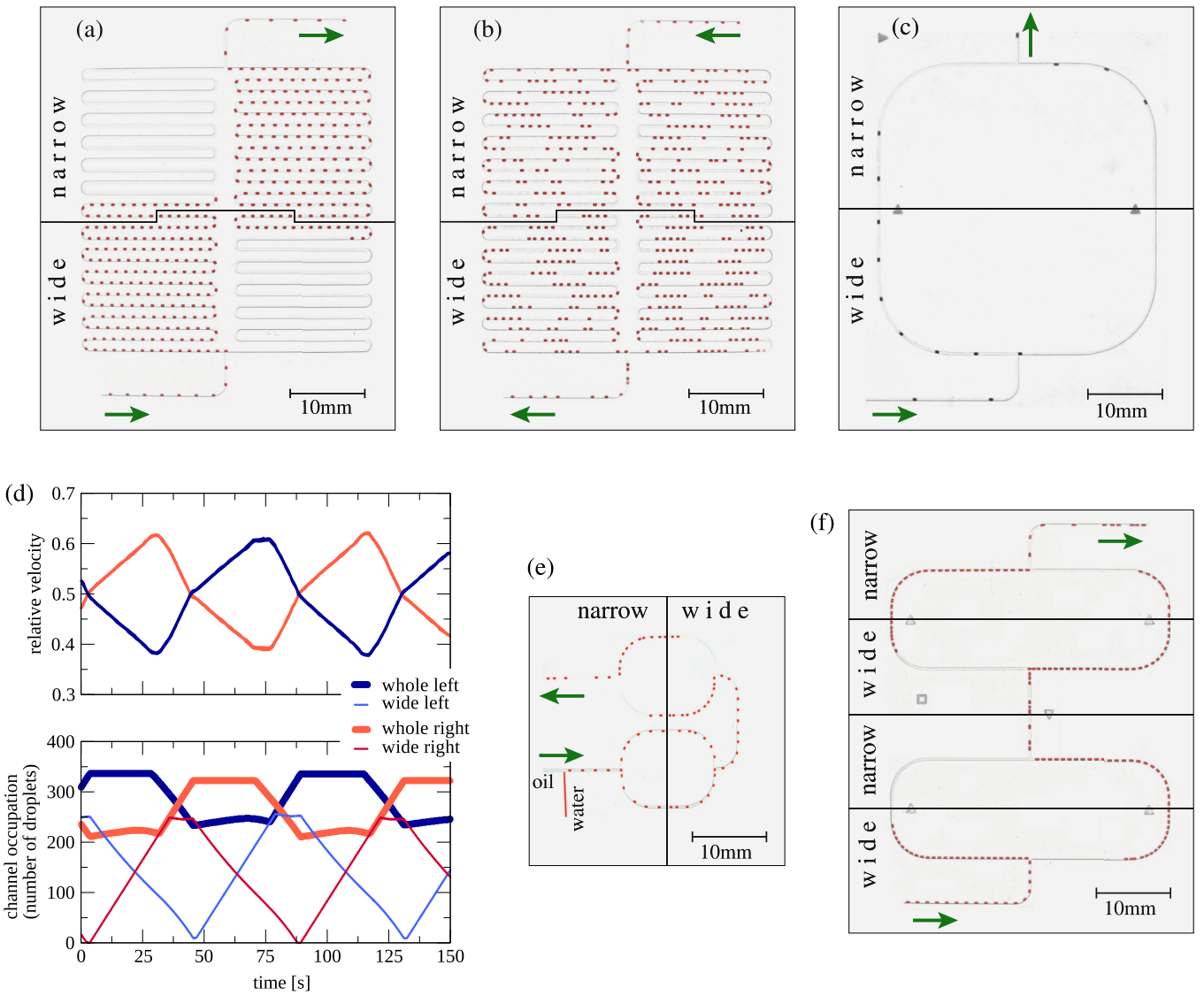


FIG. 7. (Color online) Snapshots of the experimental systems after long time of evolution at constant conditions. Direction of flow is marked with arrows. Black lines demarcate segments of channels with different cross sections, labeled as "wide" (width × height = 370 × 400 $\mu$m) and "narrow" (370 × 340 $\mu$m). (a) Queuing state of the long, symmetric loop. The "wide" channels (in fact "deep") are 230 mm long, and the "narrow" (shallow) are 250 mm long. (b) The same chip with reversed flow direction. (c) Queuing state in the symmetric loop of moderate length (66 mm per channel, equally divided between shallowed and deepened sections). This is the same chip as in Fig. 3(a)–Fig. 3(c), but there with larger separation between droplets. (d) Dynamics of queuing state in the chip (a). (e) Two identical, short loops in series; the first one is flown from shallow to deep, and the second is the opposite. Each arm is 18 mm long. (f) Two identical loops in series, both flown from "wide" to "narrow," and each arm is 55 mm long.

thermally [27], are of the same width of 370 $\mu$m and differ only in height: 340 $\mu$m for the "narrow" channels and 400 $\mu$m for the "wide," with smooth, 1-mm-long, transitions between them. As working liquids we used hexadecane with 0.5% (w/w) of Span80 surfactant and water dyed with 8% (w/w) red ink (Encre Rouge/Waterman, Paris). For these liquids and channel geometries we estimate the corresponding value of $\alpha$ for droplets of the volume of 60 nl to be $\alpha \approx 2$ for the linear velocity of droplets close to 5 mm/s, as used in the presented experiments. The smooth (1-mm-long) transitions between the wide and narrow segments of the channels produce very small changes in the curvature of the droplet and the capillary pressure (of the order of tens of Pa). The chips comprised one or two symmetric loops and one or two T junctions for generating droplets. Using two generators placed on opposite ends of the loop enabled us to invert the flow direction so droplets could enter the loop starting from shallowed segments as well as from the deepened ones. Droplets could be created passively by introducing constant rates of flow of the two liquids, yet in order to increase the range of frequencies and sizes of droplets we used a DOD technique based on pressurized containers equipped with valves and long capillaries between the valves and the chip [24].

The chip presented in Figs. 7(a)–7(b) (microphotographs) and in the graph in Fig. 7(d) comprises a long loop with arms that are 48 cm long, each including 25 cm of deepened segment

and 23 cm shallowed. As long as droplet separation was large enough to avoid mutual collisions at the inlet bifurcation [7], this chip always behaved in agreement with our predictions: Droplets flowing towards shallower segments formed perfect queues, as in Fig. 7(a), whereas in the opposite direction the patterns were quasirandom, avoiding long queues—a typical example is shown in Fig. 7(b). Regardless of the initial state, the time of formation of the perfect queues was not longer than 10 cycles.

Figure 7(d) shows cyclic changes in the flow rates and in occupation of channels in the system from Fig. 7(a), with a fully developed queue. These experimental data can be qualitatively compared with the plots in Fig. 4.

Figure 7(c) presents queuing in a symmetric loop [the same as in Figs. 3(a)–3(c)] with arms of length of 66 mm (33 mm shallowed and 33 deepened). In Figs. 3(a)–3(c) the center–to–center separation of droplets at the inlet was set to 1.47 mm—as closely as possible to the limit of the collision regime [7], and in Fig. 7(c) it is 10 mm. Supporting video [28] shows the evolution of this system from the empty loop up to the fully developed queues.

Figures 7(e) and 7(f) exemplify the use of the understanding of which geometries promote or suppress queuing in constructing microfluidic systems. Each of the systems comprises two identical loops connected in series. In Fig. 7(f) both loops are traversed from the deepened to the shallowed segments, so the queues are visible in both of the loops. In Fig. 7(e) only the second loop is oriented for queuing; the first loop is oriented so the flow proceeds from the shallowed segments towards the deeper ones, so queuing is suppressed. Unlike the long and moderate loops from Figs. 7(a)–7(c), these from Fig. 7(f) could present also patterns other than perfect queuing; it is clear that noise is required to induce transitions in loops of such a small size. Notice that the effective margin of noise in the second loop is elevated by varying intervals between droplets at the output of the first loop.

## V. CONCLUSIONS

We believe that our work may shed new light on the dynamics of the flow of droplets through microfluidic networks. We demonstrated that a theoretical description [2–5,10,11] built on the ideal model [1] does not describe the effects caused by varying the cross section of a channel and the noise that is always present in real experiments. Adding a small *intentional* modification of channels may be used for turning a chaotic system into a device that reproducibly either distributes droplets uniformly between the parallel channels or forms long queues of droplets. The experiments confirmed our numerical predictions. We found that droplets flowing through a microfluidic loop comprising two channels that narrow towards the outlet group themselves spontaneously into queues of maximum possible length. This behavior is independent on any parameters of flow, provided the droplets neither break at the bifurcation nor collide there. Although the mechanism of formation of queues is related to noise, once established, the queues cannot be destroyed even by large amplitude of random perturbations in the intervals or volumes of droplets. We also demonstrated in simulation and experiments that after reversing the flow direction (i.e., when droplets flow from narrow channels into widened sections), the queues are suppressed—resulting in uniform distribution of droplets in the loop.

Our results can be used for further studies on the dynamics of flow in microfluidic networks. They can be also directly applied for randomizing flow of droplets through branches (with channels that widen in the downstream direction), for alternate directioning of long queues to one of two outputs (with narrowing channels), and for simple, low-cost generation of periodically changing difference of flow between branches. The latter may be used, for example, for scanning the processes of splitting or collisions of droplets in a T junction as a function of the difference of flow rates.

The results described here may be also helpful in understanding the flow of blood in branched systems of vascular capillaries. Interestingly, the smallest capillaries are equipped with a mechanism of regulated constrictions at the initial section of the capillary: The regulation of lumen is provided by smooth muscles called precapillary sphincters or possibly by other mechanisms called precapillary resistance [29]. Could these constrictions be the evolutionarily developed mechanism of suppressing oscillations and promoting uniform distribution of red blood cells? In fact, giant oscillations were recently found in artificial microvascular networks [30] and earlier in theoretical models of blood capillary networks [31], although they were never observed in real microvascular networks.

Oscillations similar to our finding were recently discovered in a stratified flow of two *miscible* liquids in a narrowing loop [32]. It suggests a possible existence of a common mechanism of oscillations caused by flow of complex fluids through parallel, narrowing ducts.

## ACKNOWLEDGMENTS

This project was operated within the Foundation for Polish Science Team Programme cofinanced by the EU European Regional Development Fund and within the European Research Council Starting Grant No. 279647. S.J. and O.C. acknowledge financial support from the Polish Ministry of Science under the Grant No. IP2012 015172. The authors thank Jakub Checinski, Tomasz Smolka, Szymon Bacher, and Michal Dabrowski for valuable help during their student practices.

[1] M. Schindler and A. Ajdari, Phys. Rev. Lett. **100**, 044501 (2008).
[2] O. Cybulski and P. Garstecki, Lab Chip **10**, 484 (2010).
[3] T. Glawdel, C. Elbuken, and C. Ren, Lab Chip **11**, 3774 (2011).
[4] M. Djalali Behzad, H. Seyed-allaei, and M. R. Ejtehadi, Phys. Rev. E **82**, 037303 (2010).
[5] R. Jeanneret, J.-P. Vest, and D. Bartolo, Phys. Rev. Lett. **108**, 034501 (2012).
[6] M. Belloul, W. Engl, A. Colin, P. Panizza, and A. Ajdari, Phys. Rev. Lett. **102**, 194502 (2009).
[7] M. Belloul, L. Courbin, and P. Panizza, Soft Matter **7**, 9453 (2011).

[8] E. Kadivar, S. Herminghaus, and M. Brinkmann, J. Phys. Condens. Matter **25**, 285102 (2013).
[9] H. Boukellal, S. Selimovic, Y. Jia, G. Cristobal, and S. Fraden, Lab Chip **9**, 331 (2009).
[10] D. A. Sessoms, A. Amon, L. Courbin, and P. Panizza, Phys. Rev. Lett. **105**, 154501 (2010).
[11] B. J. Smith and D. P. Gaver III, Lab Chip **10**, 303 (2010).
[12] P. Parthiban and S. A. Khan, Lab Chip **12**, 582 (2012).
[13] T. Glawdel and C. Ren, Microfluid. Nanofluid. **13**, 469 (2012).
[14] J. Maddala, S. A. Vanapalli, and R. Rengaswamy, Phys. Rev. E **89**, 023015 (2014).
[15] A. Amon, A. Schmit, L. Salkin, L. Courbin, and P. Panizza, Phys. Rev. E **88**, 013012 (2013).
[16] O. Cybulski and P. Garstecki, Phys. Rev. E **82**, 056301 (2010).
[17] M.-C. Jullien, M.-J. T. M. Ching, C. Cohen, L. Menetrier, and P. Tabeling, Phys. Fluids **21**, 072001 (2009).
[18] S. Afkhami, A. M. Leshansky, and Y. Renardy, Phys. Fluids **23**, 022002 (2011).
[19] D. R. Link, S. L. Anna, D. A. Weitz, and H. A. Stone, Phys. Rev. Lett. **92**, 054503 (2004).
[20] M. De Menech, Phys. Rev. E **73**, 031505 (2006).
[21] W. Choi, M. Hashimoto, A. K. Ellerbee, X. Chen, K. J. M. Bishop, P. Garstecki, H. A. Stone, and G. M. Whitesides, Lab Chip **11**, 3970 (2011).
[22] N. Champagne, R. Vasseur, A. Montourcy, and D. Bartolo, Phys. Rev. Lett. **105**, 044502 (2010).
[23] W. S. Wang and S. A. Vanapalli, Biomicrofluidics **8**, 064111 (2014).
[24] K. Churski, M. Nowacki, P. M. Korczyk, and P. Garstecki, Lab Chip **13**, 3689 (2013).
[25] V. Labrot, M. Schindler, P. Guillot, A. Colin, and M. Joanicot, Biomicrofluidics **3**, 012804 (2009).
[26] M. J. Jensen, G. Goranović, and H. Bruus, J. Micromech. Microeng. **14**, 876 (2004).
[27] D. Ogonczyk, J. Wegrzyn, P. Jankowski, B. Dabrowski, and P. Garstecki, Lab Chip **10**, 1324 (2010).
[28] See Supplemental Material at http://link.aps.org/supplemental/10.1103/PhysRevE.92.063008 for the video of the experiment showing the development of queues.
[29] R. Rhoades and D. Bell, *Medical Physiology: Principles for Clinical Medicine* (Lippincott Williams & Wilkins, London, 2009).
[30] O. Forouzan, X. Yang, J. M. Sosa, J. M. Burns, and S. S. Shevkoplyas, Microvasc. Res. **84**, 123 (2012).
[31] R. Carr, J. Geddes, and F. Wu, Ann. Biomed. Eng. **33**, 764 (2005).
[32] B. D. Storey, D. V. Hellen, N. J. Karst, and J. B. Geddes, Phys. Rev. E **91**, 023004 (2015).